Estrogen exhibits a biphasic effect on prostate tumor growth through the ERβ-KLF5 pathway

Yuka Nakajima[a,b]#, Asami Osakabe[b], Tsuyoshi Waku[c], Takashi Suzuki[d], Kensuke Akaogi[b], Tetsuya Fujimura[e], Yukio Homma[e], Satoshi Inoue[f,g,h], Junn Yanagisawa[a,b]

Life Science Center of Tsukuba Advanced Research Alliance (Life Sci. Cent. of TARA)[a], Graduate School of Life and Environmental Sciences[b], University of Tsukuba, Tsukuba, Ibaraki, Japan; Graduate School of Pharmaceutical Sciences, University of Tokyo, Bunkyo-ku, Tokyo, Japan[c]; Department of Pathology and Histotechnology, Graduate School of Medicine, Tohoku University, Sendai, Miyagi, Japan[d]; Departments of Urology[e], Geriatric Medicine[f], and Anti-Aging Medicine[g], Graduate School of Medicine, University of Tokyo, Bunkyo-ku, Tokyo, Japan; Division of Gene Regulation and Signal Transduction, Research Center for Genomic Medicine, Saitama Medical University, Saitama, Japan[h]

Running title: Biphasic effect of E2 on prostate tumor growth

#Address correspondence to Yuka Nakajima, nakajima@tara.tsukuba.ac.jp

Word count for the Materials and Methods: 1,383 words

Combined word count for the Introduction, Results, and Discussion: 3,456 words

Estrogens are effective in the treatment of prostate cancer; however, the effects of estrogens on prostate cancer are enigmatic. In this study, we demonstrated that estrogen (17β-estradiol, E2) has biphasic effects on prostate tumor growth. A lower dose of E2 increased tumor growth in mouse xenograft models using DU145 and PC-3 human prostate cancer cells, whereas a higher dose significantly decreased tumor growth. We found that anchorage-independent apoptosis in these cells was inhibited by E2 treatment. Similarly, *in vivo* angiogenesis was suppressed by E2. Interestingly, these effects of E2 were abolished by knockdown of either estrogen receptor β (ERβ) or Krüppel-like zinc-finger transcription factor 5 (KLF5). In addition, E2 suppressed KLF5-mediated transcription through ERβ, which inhibits pro-apoptotic *FOXO1* and pro-angiogenic *PDGFA* expression. Furthermore, we revealed that a non-agonistic ER ligand GS-1405 inhibited *FOXO1* and *PDGFA* expression through ERβ and KLF5 pathway, and regulated prostate tumor growth without ERβ transactivation. Therefore, these results suggest that E2 biphasically modulates prostate tumor formation by regulating KLF5-dependent transcription through ERβ and provide a new strategy for designing ER modulators, which will be able to regulate prostate cancer progression with minimal adverse effects due to ER transactivation.

INTRODUCTION

Prostate cancer is the most frequently diagnosed cancer and the second leading cause of cancer death in the United States and other industrialized countries (1). Prostate cancer progression is initially driven by androgens through androgen receptor (AR). Thus, androgen ablation therapy is the primary treatment approach for prostate cancer (2, 3). However, almost all patients eventually develop resistance to anti-androgen therapy, which is extremely hard to cure (4). Therefore, new molecular targets for devising novel therapies are required.

Estrogens are known to play a role in the development of the male reproductive system and prostate cancer (5, 6). The administration of estrogens has previously been extensively used in prostate cancer treatment. Early research demonstrated that estrogens exert an indirect anti-androgen action mediated through feedback inhibition of luteinizing hormone-releasing hormone and pituitary luteinizing hormone release, thereby decreasing testicular androgen levels and release (7). On the contrary, it is currently considered that estrogens modulate prostate cancer through non-androgenic pathways (7, 8). In fact, estrogen (17β-estradiol, E2) inhibits the development of androgen-insensitive prostate cancer xenografts in mice (9, 10). Moreover, clinical studies indicated that estrogenic therapies are useful for advanced and

androgen-insensitive prostate cancer (11, 12). Despite these beneficial effects, E2 has also been revealed to be a risk factor of prostate carcinogenesis. For example, several animal studies suggested that E2 could enhance prostate cancer growth (13, 14). In addition, a recent clinicopathological study indicated that circulating E2 levels were significantly elevated in patients with prostate cancer compared with those in normal age-matched patients (15). Thus, the molecular mechanisms underlying the contradictory effects of E2 on prostate cancer development are not well understood.

E2 acts as a physiological ligand for two nuclear receptor isoforms, i.e., estrogen receptor (ER) α and ERβ (16, 17). Synthetic compounds also regulate gene expression in prostate cancer cells through ERβ, which is the predominant ER subtype in those cells (18–20). Being dependent on agonistic ligands such as E2, ER directly binds to estrogen response elements (EREs) within genomic DNA to induce gene expression (classical pathway) (21). On the contrary, recent studies revealed that ERs can also regulate gene expression by interacting with other DNA-binding transcription factors, such as c-Fos/c-Jun, Sp1, and NF-κB, but not by binding directly to DNA (non-classical pathway) (22, 23). Recent reports suggested that ER ligands regulate gene expression through ERβ-dependent non-classical pathways in prostate tissues and cancer cells (23–25). We previously reported that prostate tumor growth is regulated through the

ERβ-dependent non-classical pathway with Krüppel-like zinc finger transcription factor 5 (KLF5) (25). KLF5 (also known as BTEB2 or IKLF) is a transcription factor that possesses both tumor-suppressing and tumor-promoting activities (26–28). Analysis of the associated pathway revealed that in the absence of E2, ERβ induces the KLF5-mediated expression of *FOXO1* and increases anoikis, thereby suppressing prostate tumor growth in mouse xenograft models. Conversely, E2 suppresses KLF5 transactivation through ERβ, which enhances tumor growth. However, it is unclear whether and the mechanism by which E2 regulates prostate cancer progression through ERβ and KLF5.

In this study, we demonstrated the mechanism underlying the modulation of prostate tumor formation by E2. We revealed that E2 biphasically modulates prostate tumor growth in mouse xenograft models. Our results using the non-agonistic ER ligand GS-1405 further indicated that the effect of E2 are exerted via the comprehensive regulation of *FOXO1*-mediated anoikis and *PDGFA*-mediated angiogenesis through the ERβ–KLF5 pathway. These findings may lead to the development of new therapeutic strategies for designing next-generation ER modulators.

MATERIALS AND METHODS

Cell culture and ligand treatment. Human prostate cancer DU145 and PC-3 and human embryonic kidney HEK293 cells were obtained from the Cell Resource Center for Biomedical Research, Institute of Development, Aging and Cancer (Tohoku University, Miyagi, Japan). Human prostate cancer LNCaP cells were obtained from American Type Culture Collection. DU145, PC-3, and LNCaP cells were maintained in RPMI 1640 (Nacalai Tesque) and HEK293 cells were maintained in DMEM (Sigma-Aldrich). All media were supplemented with 10% fetal bovine serum (FBS) and penicillin-streptomycin (Nacalai Tesque). The medium was exchanged to phenol red-free medium containing 10% charcoal-stripped FBS and cells were cultured for 48 h before treatment with ligands. 17β-estradiol (E2), Fulvestrant (ICI 182,780, ICI), 4-hydroxytamoxifen (OH-Tam), raloxifene (Ral) were purchased from Sigma-Aldrich. 4-(6-methyl-1,3-benzothiazol-2-yl)phenol (GS-1405, GS; code LTBB000265) was purchased from Labtest.

Tumor xenograft models. All animal experiments were performed in accordance with the guidelines for the care and use of laboratory animals at University of Tsukuba. Methods for keeping mice and tumor xenograft models have been described previously (25). Each 5–6-week-old BALB/cA-nu castrated male mouse

was injected subcutaneously with 100 μl of cell suspension (6–8 × 10^6 cells) in both flanks. Mice were subcutaneously implanted with 17β-estradiol (E2) pellets (Innovative Research of America) 0.18 mg (E2+) or 3.4 mg (E2++) 60 days release generating serum E2 concentration from 50 to 180 pg/ml or 550 to 1900 pg/ml, which were measured using Estradiol EIA kit (Cayman). GS was subcutaneously injected in the scruff of the neck. Tumor growth was monitored by measuring the tumor size using calipers; tumor volume was determined using the formula V = 1/2 × larger diameter × (smaller diameter)^2. Twenty-five to thirty-five days after implantation, tumors were excised, weighed, and fixed or stored in liquid nitrogen for later analysis.

Expression plasmids and antibodies. The pCMV5-FLAG-ERβ (WT) plasmid has been previously described (25). To generate an expression plasmid for ERβ (E305A), site-directed mutagenesis of the *ERβ* sequence in pCMV5-FLAG-ERβ (WT) was performed by polymerase chain reaction (PCR) using the primers 5′-gttggccgacaaggcgttggtacacatg-3′ and 5′-catgtgtaccaacgccttgtcggccaac-3′. cDNAs encoding full-length *PDGFA* were amplified by PCR and subcloned into the pcDNA3 plasmid (Invitrogen) containing sequences encoding a 6× *myc* sequence. Mouse anti-PDGFA (E-10; Santa Cruz) and anti-β-actin (A5316; Sigma-Aldrich) monoclonal antibodies and rabbit anti-ERβ (CT; Millipore) and anti-CD31 (PECAM-1) (sc-1506;

Santa Cruz) polyclonal antibodies were used according to the manufacturer's instructions. The rabbit polyclonal antibodies against KLF5 and ERβ were previously generated (25).

RNA interference. Methods for stable RNA interference and siRNA transfection were followed those described by Nakajima *et al* (25). To generate the shRNA retroviral supernatant, GP2-293 cells (Clontech) were cotransfected with the pVSV-G vector (Clontech) encoding envelope protein and pRETRO-SUPER (OligoEngine) vector containing the *ERβ*, *KLF5*, or *luciferase* (control) target sequence (25). DU145 or PC-3 cells were incubated with the retroviral supernatant in the presence of 8 μg/ml polybrene. The infected cells were selected with 1 μg/ml puromycin.

Quantitative real-time (qRT)-PCR assay. The qRT-PCR assay was performed as described previously (25), with minor modifications. Cells were homogenized in 1 ml of Sepasol-RNA I Super G and total RNA was extracted, according to the manufacturer's instructions (Nacalai Tesque). cDNA was synthesized from total RNA using RevatraAce reverse transcriptase (Toyobo) and oligo dT primer. Real-time PCRs were performed to amplify fragments representing the indicated mRNAs using the Thermal Cycler Dice™ TP800 (Takara) and SYBR Premix Ex Taq II

149 (Takara). mRNA levels were normalized to those of *GAPDH*. The primer sequences
150 were as follows: *FOXO1* forward primer, 5′-tcatgtcaacctatggcag-3′; *FOXO1* reverse
151 primer, 5′-catggtgcttaccgtgtg-3′; *PDGFA* forward primer, 5′-tccacgccactaagcatgtg-3′;
152 *PDGFA* reverse primer, 5′-cgtaaatgaccgtcctggtctt-3′; *KLF5* forward primer,
153 5′-atcgagatgttcgctcgtgc-3′; *KLF5* reverse primer, 5′-tttaaaggcagacactgagtcag-3′;
154 *GAPDH* forward primer, 5′-atcgtccaccgcaaatgcttcta -3′; and *GAPDH* reverse primer,
155 5′-agccatgccaatctcatcttgtt -3′.

156 **TUNEL assay under detached conditions using poly-(2-hydroxyethyl**
157 **methacrylate) (poly-HEMA) plats and using xenograft tissues.** One gram of
158 poly-HEMA (Sigma-Aldrich) was dissolved in 25 ml of 99.5% ethanol and mixed
159 overnight at 37°C (25). The poly-HEMA stock solution was added to each well of
160 12-well plates and the plates were left to dry for a few hours. After drying, the plates
161 were washed with PBS. Cells were plated in the poly-HEMA–coated 12-well plates at
162 a density of 60,000 (PC-3) or 200,000 cells (DU145)/well and incubated for 24 h.
163 Apoptosis of the cells and xenograft tissues was analyzed by Dead End™ Fluorometric
164 TUNEL System (Promega) and the kit was used according to the manufacturer's
165 instructions.

166 **Soft agar colony formation assay.** The procedure for colony formation assay

was performed as previously described (25). In total, 22,000 cells were suspended in DMEM containing 0.35% agar (Sigma-Aldrich) and layered on top of 1 ml of DMEM solidified with 0.6% agar in each well of a six-well plate. After growing at 37°C for 4 weeks, colonies with a diameter >100 μm were observed and counted using Biozero (Keyence).

Immunohistochemical analysis. Immunohistochemistry for KLF5 was performed as previously described (25) with the following modification for CD31 and PDGFA staining. Before incubation with anti-CD31 or anti-PDGFA antibodies, antigen retrieval was performed by microwave heating in EDTA buffer (1 mM, pH 8.0) or acid buffer (2 mM citric acid and 9 mM trisodium citrate dehydrate, pH 6.0), respectively. The antigen antibody was visualized using 3,3′-diaminobenzide.

Matrigel plug angiogenesis assay. Matrigel angiogenesis experiments were performed for 7 days in 5–6-week-old castrated BALB/cA-nu mice under University of Tsukuba institutional approval. Mice were injected with 200 μl of ice-cold Matrigel (BD Biosciences) mixed with 3×10^6 cells with or without 250 ng/ml recombinant PDGFA (PeproTech). Seven days after the injection, Matrigel plugs were excised and the hemoglobin content in those plugs was determined using RIPA buffer (29).

Immunoblotting. Whole-cell lysates were extracted, and protein

185 concentrations were quantified using BCA protein assay reagent (Thermo Scientific).
186 Cell extracts were fractionated by SDS-PAGE and transferred to a polyvinylidene
187 difluoride membrane using a transfer apparatus, according to the manufacturer's
188 instructions (Bio-Rad). Antibodies used were described above. Secondary
189 antibodies were used at a concentration of 1:2000.

190 **Patients and tissues.** Tumor specimens were obtained from 102 patients who
191 provided informed consent and underwent radical prostatectomy between 1987 and
192 2001 at Tokyo University Hospital. The mean patient age was 66.0 years (range,
193 52–75 years), the mean preoperative level of prostate-specific antigen was 16.7 ng/ml
194 (3.2–136 ng/ml), and the mean follow-up period was 121 months (10–240 months).
195 Thirty-seven patients were treated with surgery alone, whereas 65 patients received
196 adjuvant anti-androgen therapy. This study was approved by the ethics committee at
197 Graduate School of Medicine, University of Tokyo (permission number 2283).

198 **Immunohistochemical assessment.** The immunoreactivity of KLF5 and
199 PDGFA was evaluated in more than 1000 carcinoma cells for each case, and
200 subsequently, the percentage of immunoreactivity, i.e., labeling index, was determined.
201 Cases with cytoplasmic staining of PDGFA in more than 10% carcinoma cells were
202 considered high immunoreactivity in this study.

Luciferase reporter assay. For luciferase assays, cells were cotransfected with phRG(R2.2)-Basic (Promega) and FX-luc, or ERE-TATA-luc (25) with or without wild type or mutated ERβ expression plasmids. Twenty-four hours after transfection, we replaced the culture medium with fresh medium containing ligands. Twenty-four hours after incubation with the ligands, luciferase assays were performed on cell extracts using a Dual-luciferase Reporter Assay System (Promega), according to the manufacturer's instructions.

Structural modeling and description of the ERβ ligand-binding domain (LBD) in complex with GS. The AutoDock Vina program (30) and AutoDock tools (31) were used for the modeling of the ligand-receptor complex. The protein structure of the hERβ LBD in complex with genistein was downloaded from the Protein Databank (PDB code: 1QKM) (32). The exact conformation of hERβ LBD in complex with GS is unclear, in particular the H12 configuration. Therefore, the H12-deleted hERβ LBD was used to the docking simulation to avoid the confusion. The model structure was described using UCSF Chimera software (33).

Chromatin immunoprecipitation (ChIP). This assay was conducted as described previously (25). The purified DNA was analyzed to determine which DNA fragments were present in the precipitate by qRT-PCR, as described above. The

primers for qRT-PCR were as follows: 5′-ccagcccggcgcccactggc-3′ and 5′-cagcggctgctgcgactacc-3′ for the *FOXO1* upstream region (25) and 5′-gcactggagggtgggcaagc-3′ and 5′-gacccgcacctcggaagcgc-3′ for the *PDGFA* upstream region.

Statistics. Statistical significance was evaluated using one-way analysis of variance for multiple groups, followed by Tukey's post hoc test to evaluate differences. Cancer-specific survival rates were evaluated based on Kaplan–Meier methods and statistical significance was determined using a log-rank test.

RESULTS

E2 exerts biphasic effects on prostate tumors growth *in vivo.* Estrogens are known to regulate prostate cancer progression, although it remains controversial whether estrogens enhance or suppress prostate cancer growth through non-androgenic pathways (7, 8). To clarify this point, we first evaluated the dose effect of E2 on prostate tumor formation by xenograft models using AR-negative DU145 or PC-3 prostate cancer cells, which express only ERβ or both ER subtypes (25, 34, 35). Consistent with previously reported results (25), mice exposed to E2 pellets (E2+) developed larger tumors

239 compared with mice treated with placebo pellets (Fig. 1A). Surprisingly, mice
240 exposed to pellets containing a higher dose of E2 (E2++) had smaller tumors than those
241 treated with placebo pellets (Fig. 1A). Then, we investigated whether E2 biphasically
242 regulated gene expression related to tumor growth. To address this, we next
243 investigated the expression levels of *FOXO1*, which acts as a tumor suppressor in
244 prostate cancer by inducing apoptosis and which is inhibited by E2 (25, 36). In cell
245 lines and xenograft tumors, the expression levels of *FOXO1* mRNA were reduced by
246 treatment with both doses of E2 (Fig. 1B and C). The percentages of TUNEL-positive
247 cells were also reduced by E2 treatment in xenograft tumors (Fig. 1D) and in DU145
248 and PC-3 cells which were cultured under anchorage-independent conditions (Fig. 1E).
249 Moreover, an *in vitro* colony formation assay revealed that the anchorage-independent
250 growth of DU145 or PC-3 cells was enhanced by E2 treatment (Fig. 1F). These results
251 indicate that E2 has a biphasic effect on prostate cancer cell growth *in vivo* but not *in*
252 *vitro*.
253
254 **E2 suppresses *in vivo* angiogenesis and regulates tumor growth through ERβ and**
255 **KLF5.** Angiogenesis plays an essential role during *in vivo* tumor growth (37, 38).
256 Thus, we investigated whether angiogenesis is involved in the molecular mechanism

underlying the biphasic effect of E2 on prostate tumor growth. We assessed vascular density in xenograft tumors via immunohistochemical staining for the endothelial cell marker CD31 and observed that the CD31-positive area was reduced in an E2 concentration-dependent manner (Fig. 2A). Then, we investigated the anti-angiogenic activity of E2 using an *in vivo* Matrigel plug angiogenesis assay. DU145 or PC-3 cells were mixed with Matrigel and subcutaneously injected into mice, which were treated with or without E2. Compared with Matrigel alone, Matrigel plugs containing DU145 or PC-3 cells had a higher hemoglobin concentration (Fig. 2B). When Matrigel-implanted mice were treated with E2, hemoglobin levels in Matrigel-containing prostate cancer cells were reduced. These results indicate that E2 inhibits *in vivo* angiogenesis induced by prostate cancer cells.

We previously showed that E2 reduces KLF5 protein levels and inhibits KLF5-mediated anoikis in DU145 and PC-3 cells through ERβ (25). We confirmed that KLF5 protein levels were reduced by E2 treatment in xenograft tumors (Fig. 2C). To further investigate whether ERβ and KLF5 are responsible for the E2-dependent modulation, we first performed a Matrigel plug assay using DU145 cells in which either ERβ or KLF5 was stably knocked down by shRNA (Fig. 2D). Knockdown of ERβ or KLF5 decreased hemoglobin levels and abolished the effects of E2 on angiogenesis (Fig.

2E), indicating that both ERβ and KLF5 are necessary for the promotion and E2-mediated inhibition of *in vivo* angiogenesis. Next, we investigated the possibility that the ERβ and KLF5 pathway contributes to the biphasic effect of E2 on prostate tumor growth using xenograft models of shERβ and shKLF5 cells. The effect of E2 on xenograft tumor growth was abolished by ERβ or KLF5 knockdown (Fig. 2F). In addition, the reduction in *FOXO1* mRNA levels by E2 treatment was not observed in shERβ or shKLF5 xenografts (Fig. 2G). These data indicate that E2 modulates prostate tumor growth through the ERβ and KLF5 pathway.

KLF5 knockdown inhibits both anoikis and angiogenesis, and exhibits biphasic effects on prostate tumor growth. To assess the *in vitro* and *in vivo* effects of KLF5 reduction on prostate tumor growth, we generated DU145 cell lines, shKLF5± and shKLF5−, in which KLF5 expression was reduced by approximately 50% and 90%, respectively (Fig. 3A and B). The levels of *FOXO1* mRNA and the number of anchorage-independent apoptotic cells were decreased in shKLF5± and shKLF5− cells (Fig. 3C and D). Interestingly, the vascularization in Matrigel plugs containing those cells was decreased by both levels of KLF5 knockdown (Fig. 3E). On the contrary, xenograft tumor growth was biphasically altered (Fig. 3F). Similar results were

293 obtained from experiments using cell lines in which KLF5 expression was reduced by
294 other shRNA target sequences (data not shown). Taken together, our observations
295 suggest that KLF5 exerts opposing functions on prostate tumor formation through
296 inhibiting anoikis and angiogenesis.
297
298 **PDGFA is involved in the inhibitory effect of KLF5 on prostate tumor growth**
299 **through angiogenesis.** To identify a KLF5 target gene that promotes angiogenesis
300 induced by prostate cancer cells, we focused on *PDGFA* because this gene is regulated
301 by KLF5, which plays a significant role in angiogenesis (39, 40). We first revealed
302 that *PDGFA* mRNA levels were decreased together with a reduction of KLF5
303 expression in DU145 cells and tumors (Fig. 4A and B). Next, we validated the effect
304 of PDGFA on *in vivo* angiogenesis through KLF5. To address this point, we injected
305 Matrigel containing shKLF5− cells mixed with or without PDGFA protein into mice
306 and observed that PDGFA recovered hemoglobin levels suppressed by KLF5 depletion
307 (Fig. 4C). Alternatively, we restored PDGFA levels in shCont. or shKLF5− cells by
308 introducing myc-tagged PDGFA expression vectors (Fig. 4D) and injected these cells
309 into mice. PDGFA expression in shCont. cells (shCont. + PDGFA) did not markedly
310 modulate xenograft tumor growth compared with the growth of control tumors (shCont.

311 + EGFP) (Fig. 4E). On the other hand, PDGFA expression in shKLF5− cells
312 (shKLF5− + PDGFA) promoted tumor formation compared with those of shKLF5− +
313 EGFP tumors. In shKLF5− tumors, the ratio of CD31-positive region was recovered
314 by PDGFA expression, but the ratio of TUNEL positive cells was not significantly
315 changed (Fig. 4F and G). Therefore, these results suggest that PDGFA is important
316 for the inhibitory effect of KLF5 on prostate tumor growth through angiogenesis.

317 Immunohistochemical staining of human prostate cancer tissues revealed that
318 FOXO1 expression levels were positively correlated with KLF5 positivity and favorable
319 cancer-specific survival in patients with prostate cancer (25). We first
320 immunohistochemically tested (Fig. 4H) the correlation between KLF5
321 immunoreactivity and PDGFA expression levels in prostate cancer tissues. KLF5
322 immunoreactivity was higher in tumor samples expressing high levels of PDGFA than
323 in samples expressing low levels of PDGFA (Fig. 4I; $P = 0.0475$), suggesting a positive
324 correlation between the abundance of KLF5 and the expression levels of PDGFA.
325 Next, we investigated the relationships between PDGFA immunoreactivity and the
326 cancer-specific survival rate of patients with prostate cancer using the Kaplan–Meier
327 method. Patients with low PDGFA-expressing tumors had higher cancer-specific
328 survival rates than patients with high PDGFA-expressing tumors (Fig. 4J; $P = 0.02$),

329 indicating that PDGFA expression is negatively correlated with the prognosis of
330 patients with prostate cancer.
331
332 **E2 suppresses angiogenesis by inhibiting *PDGFA* expression through ERβ and**
333 **KLF5.** We next examined the inhibitory effect of E2 on angiogenesis that is mediated
334 through PDGFA expression. E2 treatment decreased *PDGFA* mRNA levels in DU145
335 cells and its xenograft tumors (Fig. 5A and B). Then, we investigated whether ERβ
336 and KLF5 are also responsible for the E2-dependent suppression of *PDGFA* expression.
337 The E2-dependent reduction of *PDGFA* mRNA levels was abrogated by knockdown of
338 ERβ or KLF5 (Fig. 5C and D). In the absent of E2, *PDGFA* mRNA levels were
339 reduced by ERβ knockdown (Fig. 5C and D), supporting a role for unliganded ERβ as a
340 coactivator of KLF5 (25). To confirm the participation of PDGFA in angiogenesis
341 inhibition by E2, we injected Matrigel containing DU145 cells mixed with or without
342 PDGFA protein into mice and observed that E2-dependent reduction of hemoglobin
343 levels was restored by PDGFA protein (Fig. 5E). Thus, our results suggest that E2
344 suppresses angiogenesis by inhibiting the ERβ- and KLF5-mediated expression of
345 *PDGFA*.
346

The non-agonistic ER ligand GS inhibits the KLF5 pathway through ERβ. Previously, we identified GS as a non-agonistic ER ligand (Fig. 6A) (25). We next investigated whether GS inhibits the ERβ and KLF5 pathway without enhancing the transactivation of ERβ.

First, we compared the effects of GS and anti-estrogens on KLF5-mediated transcription using a luciferase assay with a *FOXO1*-promoter reporter construct containing KLF5-binding sites (FX-luc) (25). As anti-estrogens, we used two selective estrogen receptor modulators, 4-hydroxytamoxifen (OH-Tam) and raloxifene (Ral), and one pure ER antagonist ICI 182,780 (ICI). Consistent with the findings of our previous study (25), E2 inhibited KLF5-mediated transcription through ERβ, whereas ICI enhanced *FOXO1* promoter activity in DU145 cells (Fig. 6B). We also observed that GS inhibited the activity in a manner similar to that of E2. On the other hand, OH-Tam and Ral did not affect the activity. To validate whether GS functions through ERβ and KLF5, we additionally performed the FX-luc assay using shERβ and shKLF5 cells and showed that the inhibitory effect of GS was abolished by ERβ or KLF5 knockdown (Fig. 6C). Then, we performed docking simulation between GS and the LBD of human ERβ (hERβ LBD). In the model structure, GS formed a hydrogen bond network involving Glu305, Arg346, and a water molecule in the LBD (Fig. 6D).

365 Because these ligand–LBD interactions are important for the ERE-mediated
366 transcription of ERβ induced by E2 (Fig. 6E) (41, 42), we introduced a point mutation
367 in Glu305. We confirmed that in contrast to E2, GS did not enhance ERE-mediated
368 transcription (Fig. 6E). The E305A mutation reduced the E2- and GS-induced
369 transcriptional inhibition of *FOXO1* promoter activity (Fig. 6F), confirming the
370 inhibitory effects of these ligands on KLF5-mediated transcription through ERβ.

371 Emerging studies have demonstrated that AR plays a critical role in prostate
372 cancer development and progression, even after castration (43, 44). Therefore, we
373 investigated whether E2 and GS suppress KLF5-mediated transcription in the presence
374 of AR using AR-positive LNCaP cells, which express KLF5 and ERβ (Fig. 6G). In
375 these cells, E2 and GS inhibited *FOXO1* promoter activity, whereas the inhibitory
376 effects were abolished by KLF5 or ERβ reduction (Fig. 6H). These results suggest the
377 possibility that E2 and GS may also inhibit the KLF5 pathway through ERβ in the
378 presence of AR.

379 We then investigated the effect of GS on the mRNA levels of KLF5 target genes.
380 Similarly to E2, GS treatment decreased *FOXO1* and *PDGFA* mRNA levels but not
381 those of *KLF5* in DU145 and PC-3 cells (Fig. 7A and B). Furthermore, a ChIP
382 experiment revealed that both ligands inhibited the binding of KLF5 to the *FOXO1* or

383 *PDGFA* promoter regions containing functional or potential KLF5 response elements
384 (25, 44) (Fig. 7C and D). The inhibitory effects of E2 and GS were not observed in
385 shERβ cells.

386 Taken together, these results suggest that GS inhibits KLF5 recruitment to the
387 target promoter through ERβ for the suppression of KLF5-mediated transcription
388 without enhancing ERβ transactivation.

389

390 **GS inhibits anoikis and angiogenesis, and regulates prostate tumor growth**
391 **through ERβ.** Finally, we investigated the *in vitro* and *in vivo* effects of GS on
392 prostate tumor growth. To address this issue, we investigated whether GS affects
393 anoikis and angiogenesis. GS treatment decreased the number of apoptotic cells in
394 poly-HEMA–coated plates (Fig. 8A). In addition, GS inhibited angiogenesis in the
395 Matrigel plugs containing prostate cancer cells (Fig. 8B). Then, we used DU145 and
396 PC-3 xenograft models to evaluate the effect of GS on prostate tumor growth.
397 Compared with control mice treated with DMSO, mice treated with GS (GS+)
398 developed larger tumors, whereas those injected with a higher dose of GS (GS++) had
399 smaller tumors than control mice (Fig. 8C). We confirmed that these effects of GS
400 were abolished by ERβ knockdown (Fig. 8A–C). These results suggest that the

non-agonistic ER ligand GS inhibits anoikis and angiogenesis through ERβ and modulates prostate tumor growth.

DISCUSSION

In this study, our results address the molecular basis of the paradoxical effects of E2 in prostate cancer. Our previous results revealed that E2 treatment decreased KLF5-dependent *FOXO1* transcription in prostate cancer cells though ERβ, thereby inhibiting apoptosis and increasing tumor weight in mouse xenograft models (25). On the contrary, our present results showed that when mice were treated with higher doses of E2, prostate tumor growth was suppressed through ERβ and KLF5 in those models (Fig. 1A and 2F). We also demonstrated that E2 inhibited *PDGFA* transcription and suppressed angiogenesis through ERβ and KLF5 (Fig. 2E, 5C, and D). Moreover, PDGFA recovered angiogenesis inhibited by E2 (Fig. 5E). Apoptosis serves as a natural barrier for cancer development (45). Conversely, angiogenesis is indispensable for tumorigenesis (46). Considering the previous reports together with our data, angiogenesis may be sufficient for tumor growth in mice treated with lower doses of E2, which enhances xenograft tumor growth through the inhibition of apoptosis. On the

419 other hand, when both *PDGFA* and *FOXO1* expressions were markedly suppressed by
420 higher doses of E2, angiogenesis may be insufficient for prostate tumor growth, thereby
421 suppressing tumor growth. Therefore, our previous and present results suggest that E2
422 biphasically regulates prostate tumor growth by suppressing *FOXO1* and *PDGFA*
423 expression levels through the ERβ-KLF5 pathway (Fig. 8D).

424 In response to ligands, ERs initiate transcription by binding directly to EREs
425 (classical pathway) or by interacting with other transcription factors (non-classical
426 pathway) (22, 23). Recently, we indicated that in the absent of a ligand, ERβ acts as a
427 coactivator of KLF5 by recruiting CBP, thereby enhancing *FOXO1* expression and
428 anchorage-independent apoptosis (25). In this study, we further found that *in vivo*
429 angiogenesis was suppressed by ERβ depletion in the absent of ER ligands (Fig. 2E and
430 8B). ERβ depletion also reduced *PDGFA* mRNA levels in DU145 cells and xenograft
431 tumors that were not treated with ER ligands (Fig. 5C and D). Moreover, *PDGFA* was
432 targeted by KLF5 (Fig. 4A, 4B, and 7D) and was involved in KLF5-mediated
433 angiogenesis (Fig. 4C). Taken together, these results suggest that unliganded ERβ
434 regulates *PDGFA* expression through KLF5 transactivation and thereby mediates
435 angiogenesis *in vivo*.

436 In various cancers, including prostate cancer, KLF5 was inactivated by

437 chromosomal deletion, transcriptional silencing, and excessive protein degradation,
438 thereby suggesting that KLF5 acts as a tumor suppressor (47–50). On the contrary, in
439 prostate cancer cells, KLF5 levels are most often decreased as a result of hemizygous
440 deletion; *KLF5* is hardly deleted homozygously (49). Thus, these observations raise
441 the possibility that KLF5 both possesses a tumor suppressive function and is also
442 necessary for tumor formation. In this study, we illustrated by knockdown
443 experiments that an approximately 50% reduction of KLF5 expression in DU145 cells
444 inhibited apoptosis under anchorage-independent conditions (Fig. 3D; shKLF5±). The
445 ratio of apoptosis was more strongly suppressed by a severe reduction of KLF5
446 expression (Fig. 3D; shKLF5−). Although these results suggest that shKLF5− cells
447 possess the potential to form larger tumors than shKLF5± cells, we unexpectedly found
448 that shKLF5− cells did not form tumors in mice (Fig. 3F). In contrast, Matrigel plug
449 assays indicated that KLF5 knockdown reduced angiogenesis (Fig. 3E). Considering
450 that angiogenesis plays an indispensable role in tumorigenesis (51, 52), our results
451 suggest that prostate cancer cells, in which *KLF5* has been homozygously deleted, may
452 not be able to form tumors because of inhibited angiogenesis.

453 KLF5 is involved in cancer development in a number of human tissues, although
454 its function remains controversial (26, 27). For instance, expression of KLF5

455 enhances cell proliferation in untransformed cells and transformed fibroblasts, whereas
456 KLF5 suppresses cell growth in some cancer cells (28). Recent reports disclosed that
457 xenograft tumor growth was suppressed by the expression of wild-type KLF5 but
458 enhanced by the expression of a deacetylated KLF5 mutant (K369R) in prostate cancer
459 cells, suggesting that the roles of KLF5 are regulated by post-transcriptional
460 modifications (53). It is also known that KLF5 activity is regulated by steroid
461 hormones in breast cancer cells (54, 55). In fact, we found in this study that ER
462 ligands inhibited KLF5-mediated transcription in prostate cancer cells (Fig. 6) and
463 altered xenograft tumor growth (Fig. 1A and 8C). Thus, specific roles of KLF5 in
464 cancer development appear to be context-dependent, including post-transcriptional
465 modifications and hormone levels. Therefore, further studies are needed to address the
466 mechanism underlying the modulation of prostate cancer tumorigenesis by KLF5.

467 Estrogens, including the synthetic estrogen diethylstilbestrol, have previously
468 been used in prostate cancer treatment; however, adverse effects limited their use (8, 56).
469 These undesirable effects of estrogenic drugs are probably mediated in part by the
470 transactivation of ERs (classical pathway) (57). Our previous and present results
471 showed that E2 enhanced the transcriptional activity of ERβ and suppressed that of
472 KLF5, whereas the non-agonistic ER ligand GS inhibited KLF5-mediate transactivation

through ERβ (Fig. 6) (25). We further revealed that high-dose GS inhibited angiogenesis and prostate tumor growth in mouse xenograft models through ERβ (Fig. 8B and C). These results suggest that selective inhibition of KLF5 activity via ERβ could be useful in prostate cancer therapies that minimize adverse effects caused by ER transactivation through the classical pathway. Previous reports indicated that ERs bind to and modulate the transcriptional activity of several transcription factors, including Sp1, NF-κB, and AP1 (23, 58, 59). According to our results, it is possible to develop compounds that regulate these transcription factors separately. Therefore, our results provide a new strategy for designing next-generation ER modulators that can regulate non-classical pathways without affecting the classical pathway.

ACKNOWLEDGMENTS

We sincerely thank Prof. A. Fukamizu for a critical reading of the manuscript and helpful scientific input. We are also grateful to Dr. N. Ohnuma for valuable discussions and technical advice.

This work was supported by a Grant-in Aid for Young Scientists (B) from the Japan Society for the Promotion of Science (23790075 to YN), the research program of

the Project for Development of Innovative Research on Cancer Therapeutics (P-Direct), Ministry of Education, Culture, Sports, Science and Technology of Japan (to JY), and the Open Innovation Core (OIC) project (Yuka Nakajima; a member of OIC) of Life Science Center, Tsukuba Advance Research Alliance (TARA), University of Tsukuba, Japan.

REFERENCES

1. Siegel R, Naishadham D, Jemal A. 2013. Cancer statistics, 2013. CA Cancer J Clin 62: 11-30.
2. Ockrim J, Lalani el-N, Abel P. 2005. Therapy insight: parental estrogen treatment for prostate cancer-a new dawn for an old therapy. Nat Clin Pract Oncol 3: 552-563.
3. Shafi AA1, Yen AE, Weigel NL. 2013. Androgen receptors in hormone-dependent and castration-resistant prostate cancer. Pharmacol Ther 140: 223-238.
4. Karantanos T, Corn PG, Thompson TC. 2013. Prostate cancer progression after androgen deprivation therapy: mechanism of castrate resistance and novel therapeutic approaches. Oncogene 32: 5501-5511.
5. Ellem SJ, Risbridger GP. 2010. Aromatase and regulating the estrogen:androgen

509 ratio in the prostate gland. J. Steroid Biochem Mol Biol 118: 246-251.

510 6. Ho SM, Lee MT, Lam HM, Leung YK. 2011. Estrogens and prostate cancer:
511 etiology, mediators, prevention, and management. Endocrinol Metab Clin North Am
512 40:591-614.

513 7. Nelles JL, Hu WY, Prins GS. 2011. Estrogen action and prostate cancer. Expert Rev
514 Endocrinol Metab 6: 437-451.

515 8. Harkonen PL, Makela SI. 2004. Role of estrogens in development of prostate cancer.
516 J Steroid Biochem Mol Biol 92: 297-305.

517 9. Corey E, Quinn JE, Emond MJ, Buhler KR, Brown LG, Vessella RL. 2002.
518 Inhibition of androgen-independent growth of prostate cancer xenografts by
519 17β-estradiol. Clin Cancer Res 8: 1003-1007.

520 10. Coleman IM, Kiefer JA, Brown LG, Pitts TE, Nelson PS, Brubaker KD, Vessella
521 RL, Corey E. 2006. Inhibition of androgen-independent prostate cancer by
522 estrogenic compounds is associated with increased expression of immune-related
523 genes. Neoplasia 8: 862-878.

524 11. Ravery V, Fizazi K, Drouet L, Eymard JC, Culine S, Gravis G, Hennequin C,
525 Zerbib M. 2011. The use of estramustine phosphate in the modern management of
526 advanced prostate cancer. BJU Int 108: 1782-1786.

12. Clemons J1, Glodé LM, Gao D, Flaig TW. 2013. Low-dose diethylstilbestrol for the treatment of advanced prostate cancer. Urol Oncol 31: 198-204.

13. Ho SM. 2004. Estrogens and anti-estrogens: key mediators of prostate carcinogenesis and new therapeutic candidates. J Cell Biochem 91: 491-503.

14. Bonkhoff H, Berges R. 2009. The evolving role of oestrogens and their receptors in the development and progression of prostate cancer. Eur Urol 55: 533-542.

15. Abd Elmageed ZY, Moroz K, Srivastav SK, Fang Z, Crawford BE, Moparty K, Thomas R, Abdel-Mageed AB. 2013. High circulating estrogens and selective expression of ERβ in prostate tumors of Americans: implications for racial disparity of prostate cancer. Carcinogenesis 34: 2017-2023.

16. Kulper GG, Enmark E, Pelto-Huikko M, Nilsson S, Gustafsson JA. 1996. Cloning of a novel receptor expressed in rat prostate and ovary. Proc Natl Acad Sci USA 93: 5925-5930.

17. Shao W, Brown M. 2004. Advances in estrogen receptor biology: prospects for improvements in targeted breast cancer therapy. Breast Cancer Res 6: 39-52.

18. Enmark E, Pelto-Huikko M, Grandien K, Lagercrantz S, Lagercrantz J, Friend G, Nordenskjöld M, Gustafsson JÅ. 1997. Human estrogen receptor beta-gene structure, chromosomal localization, and expression pattern. J Clin Endocrinol Metab 82:

4258-4265.

19. Bosland MC. 2005. The role of estrogens in prostate carcinogenesis: a rationale for chemoprevention. Rev Urol 3: S4-S10.

20. McPherson SJ, Hussain S, Balanathan P, Hedwards SL, Niranjan B, Grant M, Chandrasiri UP, Toivanen R, Wang Y, Taylor RA, Risbridger GP. 2010. Estrogen receptor-β activated apoptosis in benign hyperplasia and cancer of the prostate is androgen independent and TNFα mediated. Proc Natl Acad Sci 107:3123-3128.

21. Carroll JS, Brown M. 2006. Estrogen receptor target gene: an evolving concept. Mol Endocrinol 20: 1707-1714.

22. McDevitt MA, Glidewell-Kenney C, Jimenez MA, Ahearn PC, Weiss J, Jameson JL, Levine JE. 2008. New insights into the classical and non-classical actions of estrogen: evidence from estrogen receptor knock-out and knock-in mice. Mol Cell Endocrinol 290: 24-30.

23. Leung YK, Ho SM. 2011. Estrogen receptorβ: switching to a new partner and escaping from estrogen. Sci Signal 4: pe19.

24. Leung YK, Gao Y, Lau KM, Zhang X, Ho SM. 2006. ICI 182,780-regulated gene expression in DU145 prostate cancer cells is mediated by estrogen receptor-beta/NFkappaB crosstalk. Neoplasia 8: 242-249.

563 25. Nakajima Y, Akaogi K, Suzuki T, Osakabe A, Yamaguchi C, Sunahara N, Ishida J,
564 Kako K, Ogawa S, Fujimura T, Homma Y, Fukamizu A, Murayama A, Kimura K,
565 Inoue S, Yanagisawa J. 2011. Estrogen regulates tumor growth through a
566 nonclassical pathway that includes the transcription factors ERβ and KLF5. Sci
567 Signal 4: ra22.
568 26. Dong JT, Chen C. 2009. Essential role of KLF5 transcription factor in cell
569 proliferation and differentiation and its implications for human diseases. Cell Mol
570 Life Sci 66: 2691-2706.
571 27. Simmen RC1, Pabona JM, Velarde MC, Simmons C, Rahal O, Simmen FA. 2010.
572 The emerging role of Krüppel-like factors in endocrine-responsive cancers of
573 female reproductive tissues. J Endocrinol 204: 223-231.
574 28. Diakiw SM, D'Andrea RJ, Brown AL. 2013. The double life of KLF5: Opposing
575 role in regulation of gene-expression, cellular function, and transformation. IUBMB
576 Life 65: 999-1011.
577 29. Greenberg JI, Shields DJ, Barillas SG, Acevedo LM, Murphy E, Huang J, Scheppke
578 L, Stockmann C, Johnson RS, Angle N, Cheresh DA. 2008. A role for VEGF as a
579 negative regulator of pericyte function and vessel maturation. Nature 456: 809-813.
580 30. Trott O, Olson AJ. 2010. AutoDock Vina: improving the speed and accuracy of

581 docking with a new scoring function, efficient optimization, and multithreading. J
582 Comput Chem 31: 455-461.
583 31. Himmel DM, Gourinath S, Reshetnikova L, Shen Y, Szent-Gyorgyi AG, Cohen C.
584 2002. Crystallographic findings on the internally uncoupled and near-rigor states of
585 myosin: further insights into the mechanics of the motor. Proc Natl Acad Sci USA
586 99: 12645-12650.
587 32. Sanner MF. 1999. Python: a programming language for software integration and
588 development. J Mol Graph Model 17: 57-61.
589 33. Pettersen EF, Goddard TD, Huang CC, Couch GS, Greenblatt DM, Meng EC,
590 Ferrin TE. 2004. UCSF Chimera--a visualization system for exploratory research
591 and analysis. J Comput Chem 25: 1605-1612.
592 34. Lau KM, LaSpina M, Long J, Ho SM. 2000. Expression of estrogen receptor (ER)-α
593 and ER-β in normal and malignant prostatic epithelial cells: regulation by
594 methylation and involvement in growth regulation. Cancer Res 60: 3175-3182.
595 35. Dey P, Ström A, Gustafsson JÅ. 2014. Estrogen receptor β upregulates FOXO3a
596 and causes induction of apoptosis through PUMA in prostate cancer. Oncogene 33:
597 4213-4225.
598 36. Huang H, Tindall DJ. 2008. Regulation of FOXO protein stability via ubiquitination

599 and proteasome degradation. Oncogene 27: 2312-2319.
600 37. Andrae J, Gallini R, Betsholtz C. 2008. Role of platelet-derived growth factors in
601 physiology and medicine. Genes Dev 22: 1276-1312.
602 38. Heldin CH. 2013. Targeting the PDGF signaling pathway in tumor treatment. Cell
603 Commun Signal 11: 97.
604 39. Shindo T, Manabe I, Fukushima Y, Tobe K, Aizawa K, Miyamoto S,
605 Kawai-Kowase K, Moriyama N, Imai Y, Kawakami H, Nishimatsu H, Ishikawa T,
606 Suzuki T, Morita H, Maemura K, Sata M, Hirata Y, Komukai M, Kagechika H,
607 Kadowaki T, Kurabayashi M, Nagai R. 2002. Krüppel-like zinc-finger transcription
608 factor KLF5/BTEB2 is a target for angiotensin II signaling and an essential
609 regulator of cardiovascular remodeling. Nat Med 8: 856-863.
610 40. Pietras K, Pahler J, Bergers G, Hanahan D. 2008. Functions of paracrine PDGF
611 signaling in the proangiogenic tumor stroma revealed by pharmacological targeting.
612 PLoS Med 5: e19.
613 41. Shi Y, Koh JT. 2002. Functionally orthogonal ligand-receptor pairs for the selective
614 regulation of gene expression generated by manipulation of charged residues at the
615 ligand-receptor interface of ER alpha and ER beta. J Am Chem Soc 124: 6921-6928.
616 42. Bertini S, De Cupertinis A, Granchi C, Bargagli B, Tuccinardi T, Martinelli A,

617 Macchia M, Gunther JR, Carlson KE, Katzenellenbogen JA, Minutolo F. 2011.
618 Selective and potent agonists for estrogen receptor beta derived from molecular
619 refinements of salicylaldoximes. Eur J Med Chem 46: 2453-2462.
620 43. Lonergan PE, Tindall DJ. 2011. Androgen receptor signaling in prostate cancer
621 development and progression. J Carcinog 10: 20.
622 44. Aizawa K, Suzuki T, Kada N, Ishihara A, Kawai-Kowase K, Matsumura T, Sasaki
623 K, Munemasa Y, Manabe I, Kurabayashi M, Collins T, Nagai R. 2004. Regulation
624 of platelet-derived growth factor-A chain by Krüppel-like factor 5: new pathway of
625 cooperative activation with nuclear factor-kappaB. J Biol Chem 279: 70-76.
626 45. Hanahan D, Weinberg RA. 2011. Hallmarks of cancer: the next generation. Cell
627 144: 646-674.
628 46. Folkman J. 2003. Angiogenesis and apoptosis. Semin Cancer Biol 13: 159-167.
629 47. Knuutila S, Aalto Y, Autio K, Björkqvist AM, El-Rifai W, Hemmer S, Huhta T,
630 Kettunen E, Kiuru-Kuhlefelt S, Larramendy ML, Lushnikova T, Monni O, Pere H,
631 Tapper J, Tarkkanen M, Varis A, Wasenius VM, Wolf M, Zhu Y. 1999. DNA copy
632 number losses in human neoplasm. Am J Pathol 155: 683-694.
633 48. Dong JT. 2001. Chromosomal deletions and tumor suppressor genes in prostate
634 cancer. Cancer Metastasis Rev 20: 173-193.

635 49. Chen C, Bhalala HV, Vessella RL, Dong. JT. 2003. KLF5 is frequently deleted and
636 down-regulated but rarely mutated in prostate cancer. Prostate 55; 81-88.
637 50. Chen C, Sun X, Ran Q, Wilkinson KD, Murphy TJ, Simons JW, Dong JT. 2005.
638 Ubiquitin-proteasome degradation of KLF5 transcription factor in cancer and
639 untransformed epithelial cells. Oncogene 24: 3319-3327.
640 51. Bergers G, Hanahan D. 2008. Modes of resistance to anti-angiogenic therapy. Nat
641 Rev Cancer 8: 592-603.
642 52. Ribeiro AL, Okamoto OK. 2015. Combined effects of pericytes in the tumor
643 microenvironment. Stem Cells Int 2015: 868475.
644 53. Li X, Zhang B, Wu Q, Ci X, Zhao R, Zhang Z, Xia S, Su D, Chen J, Ma G, Fu L,
645 Dong JT. 2015. Interruption of KLF5 acetylation converts its function from tumor
646 suppressor to tumor promoter in prostate cancer cells. Int J Cancer 136: 536-546.
647 54. Zhao KW, Sikriwal D, Dong X, Guo P, Sun X, Dong JT. 2011. Oestrogen causes
648 degradation of KLF5 by inducing the E3 ubiquitin ligase EFP in ER-positive breast
649 cancer cells. Biochem J 437: 323-333.
650 55. Liu R, Zhou Z, Zhao D, Chen C. 2011. The induction of KLF5 transcription factor
651 by progesterone contributes to progesterone-induced breast cancer cell proliferation
652 and dedifferentiation. Mol Endcrinol 25: 1137-1144.

653 56. Wibowo E, Schellhammer P, Wassersug RJ. 2011. Role of estrogen in normal male
654 function: clinical implications for patients with prostate cancer on androgen
655 deprivation therapy. J Urol 185: 17-23.
656 57. Ho SM, Leung YK, Chung I. 2006. Estrogens and antiestrogens as etiological
657 factors and therapeutics for prostate cancer. Ann N Y Acad Sci 1089:177-193.
658 58. Bjornstrom L, Sjoberg M. 2005. Mechanisms of estrogen receptor signaling:
659 convergence of genomic and nongenomic actions on target genes. Mol Endocrinol
660 19: 833-842.
661 59. Zhao C, Gao H, Liu Y, Papoutsi Z, Jaffrey S, Gustafsson JA, Dahlman-Wright K.
662 2010. Genome-wide mapping of estrogen receptor-beta-binding regions reveals
663 extensive cross-talk with transcription factor activator protein-1. Cancer Res 70:
664 5174-5183.

Figure Legends

FIG 1 17β-estradiol (E2) has a biphasic effect on prostate tumor growth. (**A**) E2 biphasically regulates tumor formation in nude mice. Mice were injected with DU145 or PC-3 cells in both flanks and implanted with a control pellet (placebo) or a pellet containing 0.18 (E2+) or 3.4 mg (E2++) of E2 (released for 60 days). Tumor growth curves are presented in left panels. After 25 or 28 days, the xenografts were removed and weighed (right panel). The middle panels show representative photographs of the tumors (scale bars, 1 cm). (**B**, **C**) E2 treatment reduces *FOXO1* mRNA levels in xenografts and prostate cancer cells. (B) *FOXO1* mRNA levels in the indicated xenograft tumors were determined by qRT-PCR. (C) DU145 or PC-3 cells were cultured in the absence (DMSO) or presence of E2 (E2+, 10 nM; E2++, 1 μM). Twelve hours after treatment, *FOXO1* mRNA levels were determined by qRT-PCR. (**D, E**) E2 inhibits apoptosis in xenografts and prostate cancer cells. (D) DU145 and PC-3 xenograft tumors were examined in TUNEL assays. (E) DU145 or PC-3 cells were seeded on poly-HEMA-coated plates in the presence of DMSO or E2 (E2+, 10 nM; E2++, 1 μM). After 24 h, the cells were examined in TUNEL assays. (**F**) E2 enhances the anchorage-independent growth of prostate cancer cells in soft agar. DU145 or PC-3 cells were plated on 0.35% soft agar plates in the presence of DMSO or

683 E2 (E2+, 10 nM; E2++, 1 μM). Colonies with a diameter of more than 100 μm were
684 counted. Values are presented as mean ± SD. n = 4–6 for A, B, and D, n = 3 for C, E,
685 and F. *, $P < 0.05$, **, $P < 0.01$.
686
687 **FIG 2 E2 modulates angiogenesis and tumor growth through ERβ and KLF5.**
688 (**A**) E2 inhibits angiogenesis in DU145 and PC-3 xenograft tumors. Paraffin sections
689 of the indicated xenograft tumors were stained with antibodies for the blood vessel
690 marker CD31, and the CD31 expression level was quantified by image analysis and
691 expressed as a percentage of the control. Scale bar, 100 μm. (**B**, **E**) E2 inhibits
692 angiogenesis induced by prostate cancer cells through ERβ and KLF5. Nude mice
693 were injected subcutaneously with Matrigel, with or without the indicated cells, and the
694 vehicle (DMSO) or E2 (E2+, 21 μg/week; E2++, 210 μg/week). Seven days after the
695 injection, the Matrigel plugs were removed from the mice and homogenized. The
696 supernatant was analyzed for hemoglobin content. The left panels show representative
697 photographs of Matrigel plugs (scale bars, 0.5 cm). (**C**) KLF5 protein levels are lower
698 in tumors from E2-treated mice. KLF5 protein levels in the indicated xenograft
699 tumors were examined by immunoblotting. (**D**) Endogenous ERβ or KLF5 expression
700 was stably suppressed in DU145 cells following the introduction of *ERβ* shRNA

(shERβ) or *KLF5* shRNA (shKLF5). Those protein levels were determined by immunoblotting. (**F**) E2 biphasically regulates tumor formation through ERβ and KLF5. Mice were injected with the indicated knockdown DU145 cells in both flanks and implanted with a placebo, E2+, or E2++ pellet. Tumor growth curves are presented in left panels. After 35 days, the xenografts were removed and weighed (right panel). (**G**) E2 reduces *FOXO1* mRNA levels in xenografts through ERβ and KLF5. *FOXO1* mRNA levels in the indicated xenograft tumors were determined by qRT-PCR. Values are presented as mean ± SD. n = 4–8 for A, B, and E to G. *, $P < 0.05$, **, $P < 0.01$; n.s., not significant.

FIG 3 KLF5 knockdown suppresses anoikis and angiogenesis and exerts opposing functions on prostate tumor growth. (**A**, **B**) KLF5 expression levels in shKLF5± and shKLF5− cells. DU145 cells were transfected with *luciferase* shRNA (shCont) or *KLF5* shRNA (shKLF5± or shKLF5−). *KLF5* mRNA (A) or protein levels (B) were determined by qRT-PCR or immunoblotting, respectively. (**C**) KLF5 knockdown reduces *FOXO1* mRNA levels in prostate cancer cells. *FOXO1* mRNA levels in the indicated cells were examined by qRT-PCR. (**D**) KLF5 knockdown inhibits anoikis in prostate cancer cells. The indicated cells were seeded on poly-HEMA-coated plates

and subjected to TUNEL assays. (**E**) KLF5 knockdown inhibits angiogenesis induced by prostate cancer cells. Hemoglobin content in plugs with or without the indicated cells was examined using a Matrigel plug assay (scale bars, 0.5 cm in the left panel). (**F**) KLF5 knockdown modulates prostate tumor growth in mice. Nude mice were injected with the indicated cells in both flanks. Tumor growth curves are presented in left panel. After 28 days, the tumors were removed and weighed (right panel). The middle panel shows representative photographs of the tumors (scale bar, 1 cm). Values are presented as mean ± SD. n = 3 for A, C, and D; n = 4–6 for E and F. *, $P < 0.05$, **, $P < 0.01$.

FIG 4 PDGFA mediates the inhibitory effect of KLF5 on prostate tumor growth through angiogenesis. (**A**, **B**) *PDGFA* mRNA levels are reduced by KLF5 knockdown. *PDGFA* mRNA levels in the indicated cells (A) or xenograft tumors (B) were determined by qRT-PCR. (**C**) PDGFA recovers angiogenesis suppressed by KLF5 knockdown. The indicated cells were mixed with Matrigel and the vehicle or PDGFA (500 ng/plug) and the mixture was subcutaneously injected into nude mice. The quantification of hemoglobin levels within Matrigel plugs is shown in the right panel. The left panel shows representative photographs of Matrigel plugs (scale bar,

737 0.5 cm). (**D**) PDGFA, KLF5, and FOXO1 expression levels in control or shKLF5−
738 cells expressing EGFP or PDGFA. DU145 cells were transfected with a combination
739 of *luciferase* shRNA and EGFP expression plasmids (shCont + EGFP), *luciferase*
740 shRNA and myc-tagged PDGFA expression plasmids (shCont. + PDGFA), *KLF5*
741 shRNA and EGFP expression plasmids (shKLF5− + EGFP), or *KLF5* shRNA and
742 myc-tagged PDGFA expression plasmids (shKLF5− + PDGFA). PDGFA, KLF5, and
743 FOXO1 protein levels were determined by immunoblotting. (**E**) PDGFA expression
744 promotes tumor formation inhibited by KLF5 knockdown. Nude mice were
745 subcutaneously inoculated in both flanks with the indicated cells. Tumor growth
746 curves are presented in left panel. After 28 days, the xenografts were removed and
747 weighed (right panel). The middle panel shows representative photographs of the
748 tumors (scale bar, 1 cm). (**F**, **G**) PDGFA expression recovers angiogenesis, but not
749 changes apoptosis ratios in KLF5 knockdown xenograft tumors. The indicated
750 xenograft tumors were examined in immunostaining of CD31 (F) or TUNEL assays (G).
751 Values are presented as mean ± SD. n = 3 for A and B; n = 4–9 for C and E to G. *,
752 $P < 0.05$, **, $P < 0.01$; n.s., not significant. (**H**) Representative prostate cancer tissues
753 labeled with anti-KLF5 and anti-PDGFA antibodies (scale bars, 50 μm). (**I**)
754 Association between the KLF5 labeling index and PDGFA expression levels in prostate

cancer tissues. Prostate cancer tissues were labeled with anti-KLF5 or anti-PDGFA antibodies. "High" and "Low" indicate samples with either high (>10% positive carcinoma cells) or low (≤10% positive carcinoma cells) PDGFA immunoreactivity. (**J**) Clinical association of PDGFA with cancer-specific survival. Cancer-specific survival rates were analyzed using the Kaplan–Meier method for high PDGFA- or low PDGFA-expressing samples.

FIG 5 E2 inhibits angiogenesis through the suppression of *PDGFA* expression. (**A** to **D**) E2 treatment reduces *PDGFA* mRNA levels through ERβ and KLF5. DU145 (A) or the indicated knockdown cells (C) were cultured in the absence (DMSO) or presence of E2 (E2+, 10 nM; E2++, 1 μM). *PDGFA* mRNA levels in the indicated cells (A, C) or tumors (B, D) were determined by qRT-PCR. (**E**) PDGFA counteracts the inhibition of angiogenesis induced by E2. Nude mice were injected subcutaneously with Matrigel, with or without DU145 cells and proteins (PDGFA, 500 ng/plug), and the vehicle or E2 (210 μg/week). Quantification of hemoglobin levels within Matrigel plugs is shown in the right panel. Representative photographs are displayed in the left panel (scale bar, 0.5 cm). Values are presented as mean ± SD. n = 3-6. *, $P < 0.05$, **, $P < 0.01$; n.s., not significant.

773

774 **FIG 6 The non-agonistic ER ligand GS inhibits KLF5-mediated transcription**
775 **through ERβ.** (**A**) Chemical structures of E2 and GS. (**B**, **C**, and **H**) E2 and GS
776 inhibit *FOXO1* promoter activity through ERβ and KLF5. A luciferase reporter
777 plasmid containing the *FOXO1* promoter (−83 to +56, FX-luc) was transfected into
778 DU145 (B and C) or LNCaP (H) cells. Cell extracts derived from cultures containing
779 E2, GS, 4-hydroxytamoxifen (OH-Tam), raloxifene (Ral), or ICI 182,780 (ICI) (1 μM)
780 were examined using luciferase assays. (**D**) GS forms the hydrogen bond with the
781 hERβ LBD in docking model. GS is represented as a ball-and-stick model (cyan),
782 whereas ligand-interacting residues are represented as sticks (light blue). Hydrogen
783 bonds between GS and the hERβ LBD are indicated as red lines. The main chain of
784 the hERβ LBD (PDB 1QKM) is represented with a cartoon model (transparent blue).
785 (**E**) E2, but not GS, enhances ERE-mediated transcription. ER-negative HEK293 cells
786 were transfected with ERE-TATA-luc and the indicated ERβ expression plasmid.
787 Transfected cells were then treated with E2 or GS (10 nM) for 24 h before the
788 preparation of extracts. Cell extracts derived from cultures were examined using
789 luciferase assays. (**F**) E305A mutation of ERβ abolishes the inhibition of *FOXO1*
790 expression by GS. FX-luc and the indicated ERβ expression plasmid were transfected

791 into HEK293 cells. Cell extracts derived from cultures containing the indicated ER
792 ligands (1 μM) were examined using luciferase assays. (**G**) Endogenous KLF5 or ERβ
793 expression was suppressed in LNCaP cells following the introduction of *KLF5* siRNA
794 (siKLF5) or *ERβ* siRNA (siERβ). Those protein levels were determined by
795 immunoblotting. Values are presented as mean ± SD. n = 3-4. **, $P < 0.01$; n.s., not
796 significant.
797
798 **FIG 7 E2 and GS suppress *FOXO1* and *PDGFA* expression through inhibiting**
799 **KLF5 interaction to those promoter regions.** (**A**) GS treatment reduces *FOXO1* and
800 *PDGFA* mRNA levels in prostate cancer cells. DU145 or PC-3 cells were cultured in
801 the absence (DMSO) or presence of GS (GS+, 10 nM; GS++, 1 μM), and *FOXO1* or
802 *PDGFA* mRNA levels were determined by qRT-PCR. (**B**) E2 or GS treatment does
803 not affect *KLF5* mRNA levels. DU145 or PC-3 cells were cultured in the absence
804 (DMSO) or presence of E2 or GS (1 μM) and *KLF5* mRNA levels were determined by
805 qRT-PCR. (**C**, **D**) E2 or GS treatment inhibits the binding of KLF5 to the *FOXO1* (C)
806 and *PDGFA* promoter regions (D) through ERβ. Control (shCont.) and ERβ
807 knockdown (shERβ) DU145 cells were cultured in the absence (DMSO) or presence of
808 the indicated ER ligands (1 μM). ChIP assays were performed using anti-KLF5

809 antibodies. Immunoprecipitated DNA was assessed in qRT-PCR assays using primers
810 specific for the *FOXO1* or *PDGFA* promoter. Samples were normalized to the input
811 DNA. Values are presented as mean ± SD. n = 3. *, $P < 0.05$; **, $P < 0.01$; n.s., not
812 significant.
813
814 **FIG 8 GS regulates prostate tumor growth through the inhibition of anoikis and**
815 **angiogenesis.** (**A**) GS suppresses anoikis in prostate cancer cells. DU145 or PC-3
816 cells were seeded onto poly-HEMA–coated plates in the presence of DMSO or GS
817 (GS+, 10 nM; GS++, 1 μM). After 24 h, the cells were examined by TUNEL assays.
818 (**B**) GS inhibits *in vivo* angiogenesis through ERβ. Hemoglobin content in plugs with
819 the indicated cells treated with or without GS (GS+, 5 mg/week; GS++, 25 mg/week)
820 was examined using a Matrigel plug assay (scale bars, 0.5 cm). (**C**) GS modulates
821 prostate tumor growth. Nude mice were injected with the indicated cells followed by
822 the vehicle (DMSO) or GS (GS+, 5 mg/week; GS++, 25 mg/week). Tumor growth
823 curves are presented in left panel. After 28 days, the tumors were removed and
824 weighed (right panels). The middle panel shows representative photographs of the
825 tumors (scale bar, 1 cm). (**D**) A schematic model of the mechanism by which E2 or
826 GS biphasically regulates prostate tumor growth. Values are presented as mean ± SD.

827 n = 3 for A; n = 4–8 for B and C. **, $P < 0.01$; n.s., not significant.

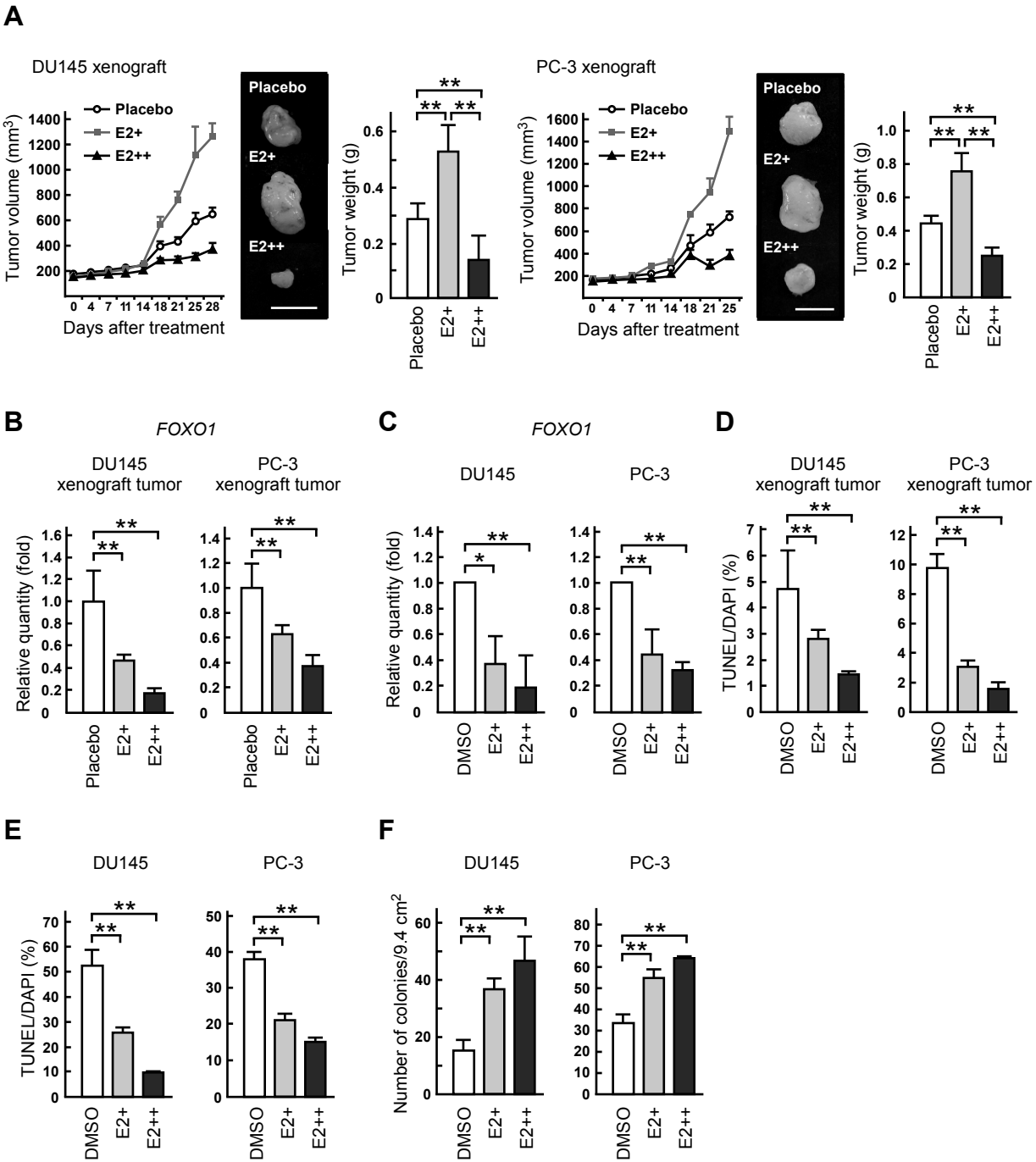
A
DU145 xenograft
Placebo
E2+
E2++
Tumor volume (mm3)
Days after treatment
Tumor weight (g)
PC-3 xenograft
B
FOXO1
DU145 xenograft tumor
PC-3 xenograft tumor
Relative quantity (fold)
C
DU145
PC-3
D
TUNEL/DAPI (%)
E
F
Number of colonies/9.4 cm2
DMSO

Figure_1

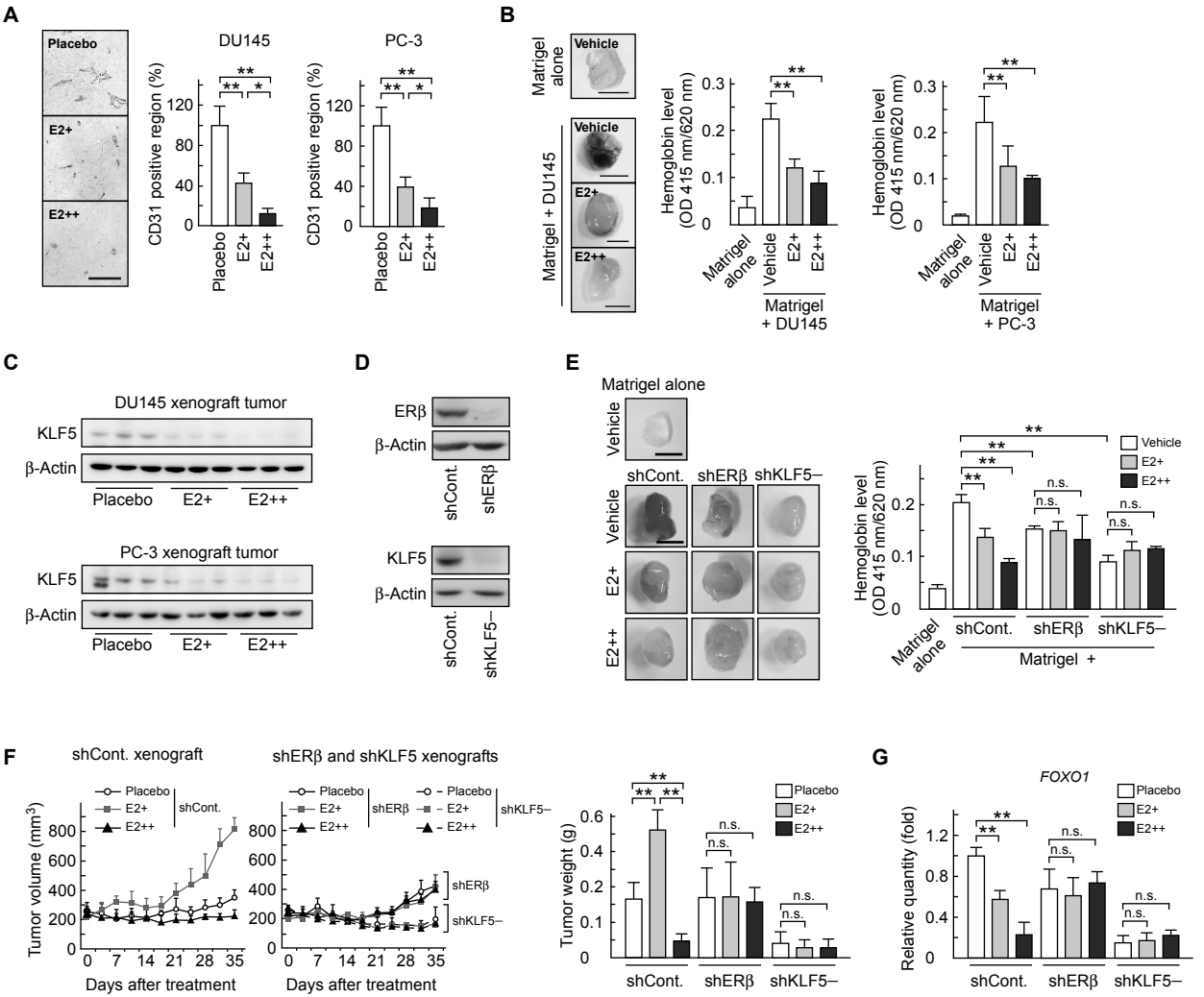
A
Placebo
E2+
E2++
DU145
PC-3
CD31 positive region (%)
Placebo
E2+
E2++
B
Matrigel alone
Matrigel + DU145
Vehicle
E2+
E2++
Hemoglobin level (OD 415 nm/620 nm)
Matrigel alone
Vehicle
Matrigel + DU145
Matrigel + PC-3
C
DU145 xenograft tumor
KLF5
β-Actin
PC-3 xenograft tumor
D
ERβ
shCont.
shERβ
shKLF5–
E
Matrigel alone
shERβ
shKLF5–
Matrigel +
F
shCont. xenograft
shERβ and shKLF5 xenografts
Tumor volume (mm3)
Days after treatment
Tumor weight (g)
G
FOXO1
Relative quantity (fold)

Figure_2

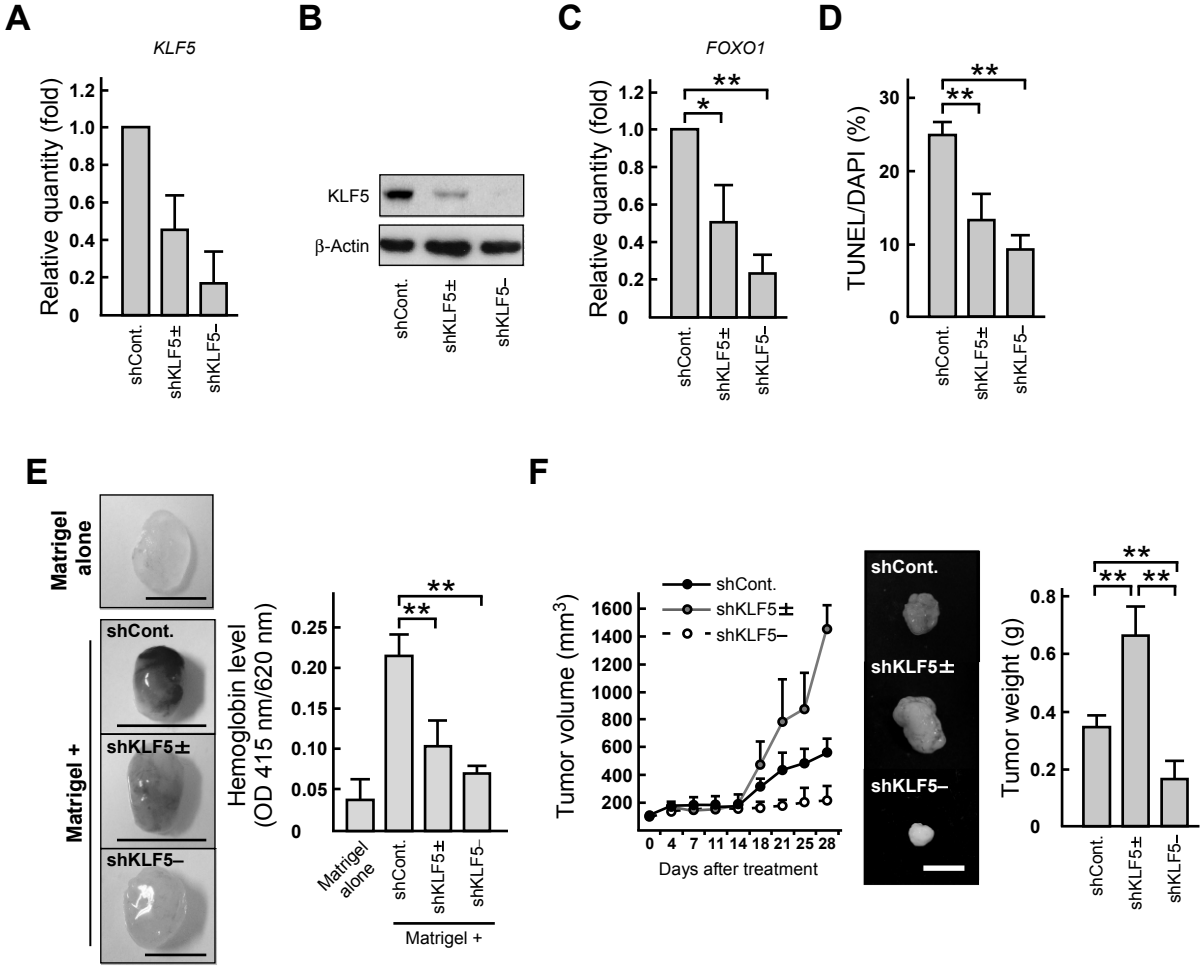
A
KLF5
Relative quantity (fold)
1.2
1.0
0.8
0.6
0.4
0.2
0
shCont.
shKLF5±
shKLF5–
B
KLF5
β-Actin
shCont.
shKLF5±
shKLF5–
C
FOXO1
Relative quantity (fold)
**
*
shCont.
shKLF5±
shKLF5–
D
TUNEL/DAPI (%)
30
20
10
0
**
**
shCont.
shKLF5±
shKLF5–
E
Matrigel alone
Matrigel +
shCont.
shKLF5±
shKLF5–
Hemoglobin level (OD 415 nm/620 nm)
0.25
0.20
0.15
0.10
0.05
0
**
**
Matrigel alone
shCont.
shKLF5±
shKLF5–
Matrigel +
F
Tumor volume (mm3)
1600
1400
1200
1000
800
600
400
200
shCont.
shKLF5±
shKLF5–
0 4 7 11 14 18 21 25 28
Days after treatment
shCont.
shKLF5±
shKLF5–
Tumor weight (g)
0.8
0.6
0.4
0.2
0
**
**
**
shCont.
shKLF5±
shKLF5–

Figure_3

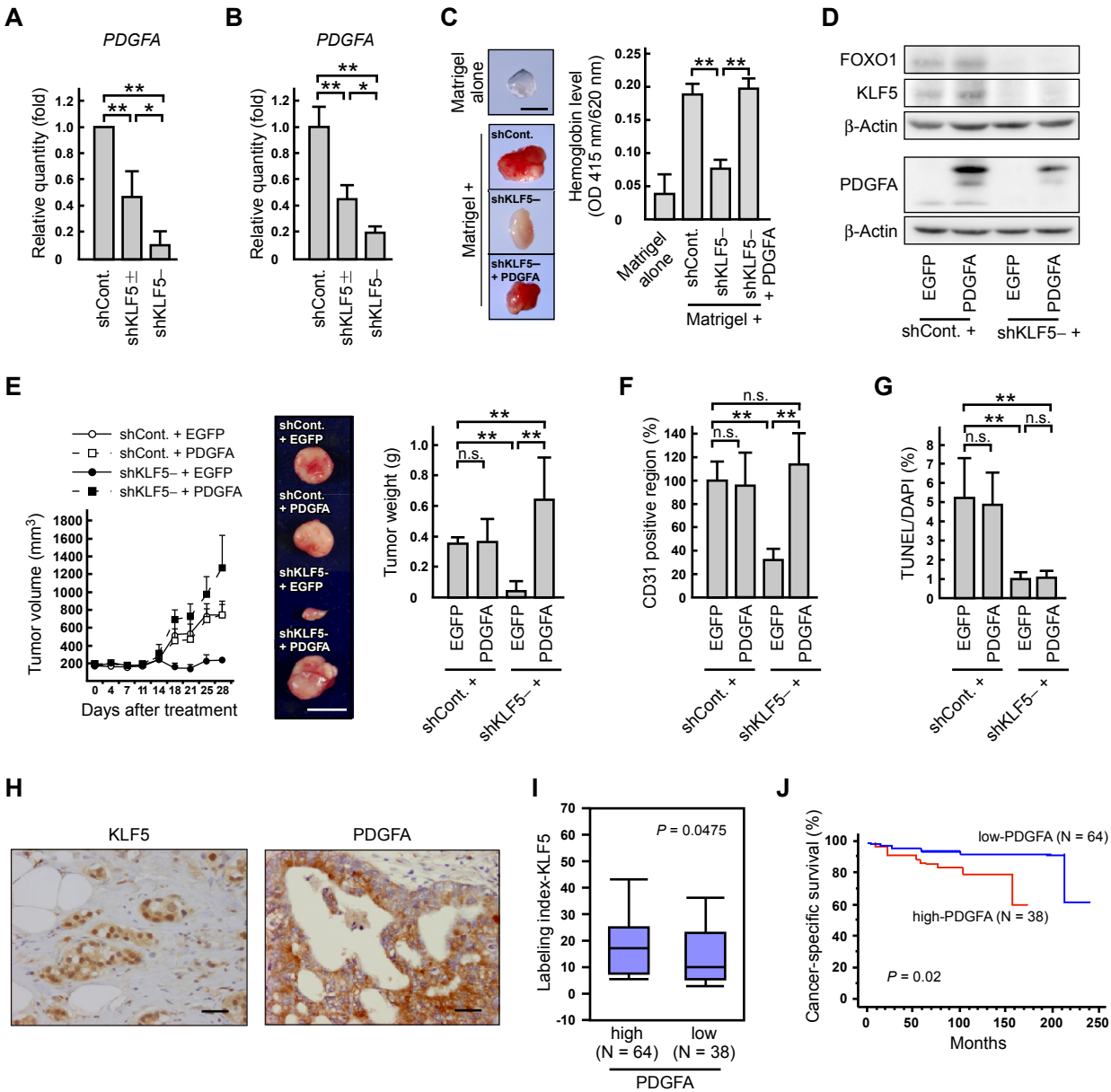
A
PDGFA
Relative quantity (fold)
shCont.
shKLF5 ±
shKLF5–
B
PDGFA
Relative quantity (fold)
shCont.
shKLF5 ±
shKLF5–
C
Matrigel alone
Matrigel +
shCont.
shKLF5–
shKLF5– + PDGFA
Hemoglobin level (OD 415 nm/620 nm)
Matrigel alone
shCont.
shKLF5–
shKLF5– + PDGFA
Matrigel +
D
FOXO1
KLF5
β-Actin
PDGFA
β-Actin
EGFP
PDGFA
EGFP
PDGFA
shCont. +
shKLF5– +
E
shCont. + EGFP
shCont. + PDGFA
shKLF5– + EGFP
shKLF5– + PDGFA
Tumor volume (mm3)
Days after treatment
shCont.
+ EGFP
shCont.
+ PDGFA
shKLF5-
+ EGFP
shKLF5-
+ PDGFA
Tumor weight (g)
n.s.
EGFP
PDGFA
EGFP
PDGFA
shCont. +
shKLF5– +
F
CD31 positive region (%)
n.s.
n.s.
EGFP
PDGFA
EGFP
PDGFA
shCont. +
shKLF5– +
G
TUNEL/DAPI (%)
n.s.
n.s.
EGFP
PDGFA
EGFP
PDGFA
shCont. +
shKLF5– +
H
KLF5
PDGFA
I
Labeling index-KLF5
P = 0.0475
high (N = 64)
low (N = 38)
PDGFA
J
Cancer-specific survival (%)
low-PDGFA (N = 64)
high-PDGFA (N = 38)
P = 0.02
Months

Figure_4

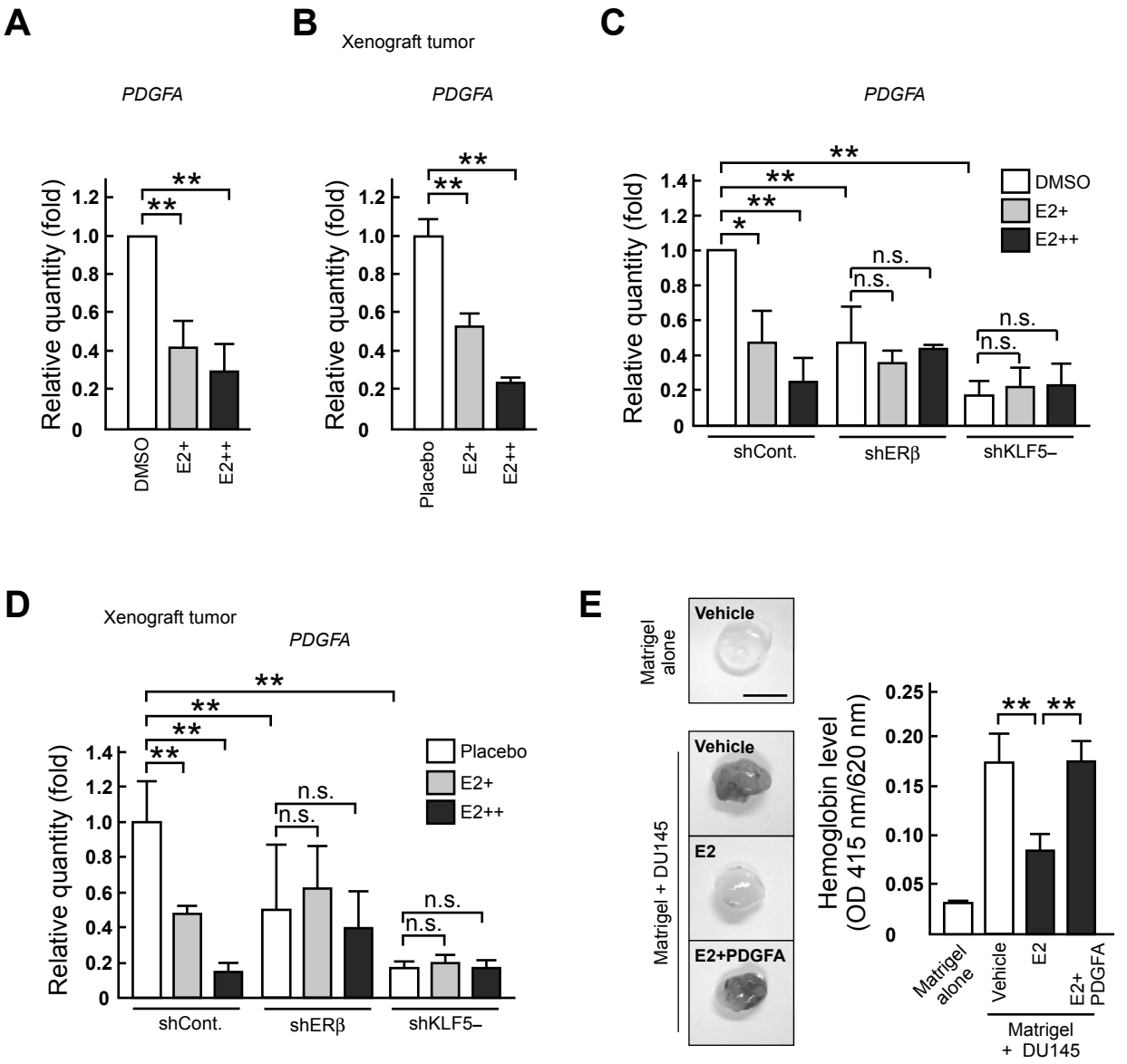
A
PDGFA
Relative quantity (fold)
DMSO
E2+
E2++
B
Xenograft tumor
PDGFA
Relative quantity (fold)
Placebo
E2+
E2++
C
PDGFA
Relative quantity (fold)
DMSO
E2+
E2++
shCont.
shERβ
shKLF5–
n.s.
D
Xenograft tumor
PDGFA
Relative quantity (fold)
Placebo
E2+
E2++
shCont.
shERβ
shKLF5–
n.s.
E
Matrigel alone
Vehicle
Matrigel + DU145
Vehicle
E2
E2+PDGFA
Hemoglobin level (OD 415 nm/620 nm)
Matrigel alone
Vehicle
E2
E2+ PDGFA
Matrigel + DU145

Figure_5

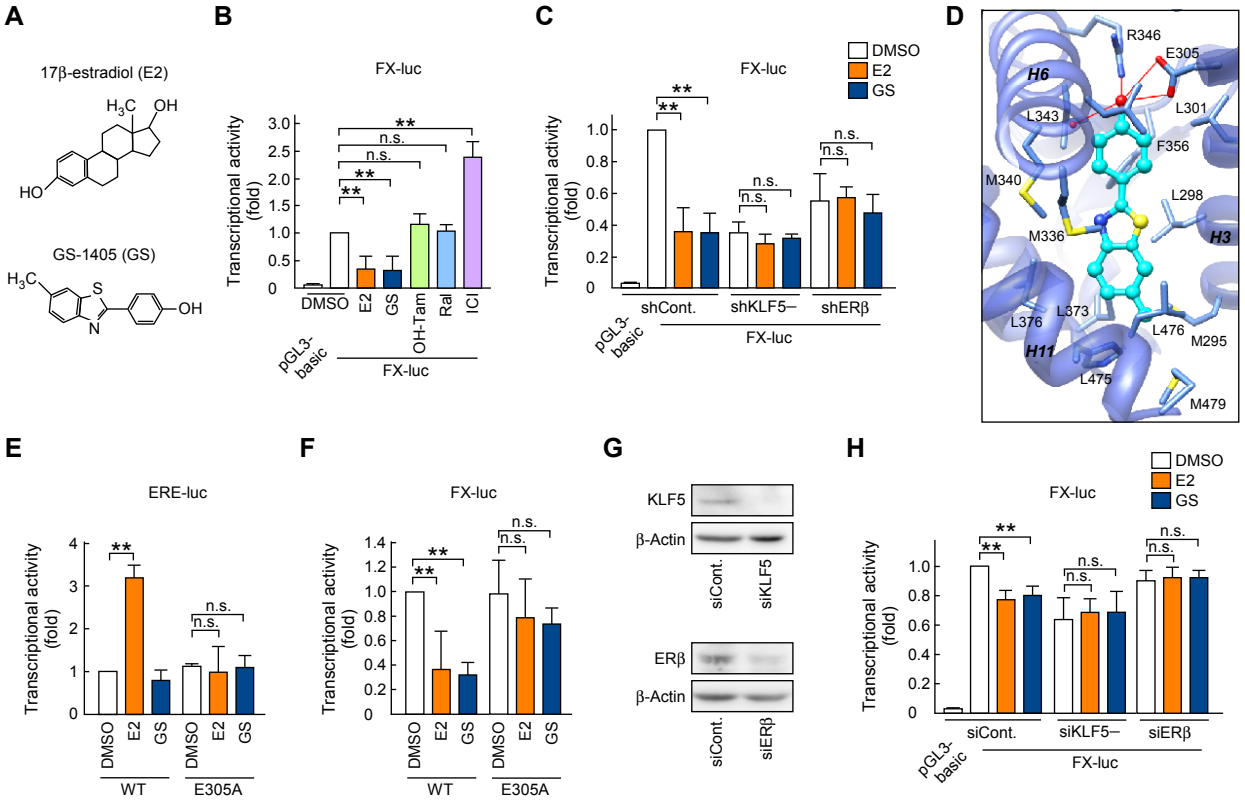
A
17β-estradiol (E2)
GS-1405 (GS)
B
FX-luc
Transcriptional activity (fold)
DMSO
E2
GS
OH-Tam
Ral
ICI
pGL3-basic
FX-luc
C
FX-luc
DMSO
E2
GS
shCont.
shKLF5
shERβ
D
R346
E305
H6
L343
L301
F356
M340
L298
M336
H3
L373
L376
L476
M295
H11
L475
M479
E
ERE-luc
WT
E305A
F
FX-luc
G
KLF5
β-Actin
siCont.
siKLF5
ERβ
siERβ
H
FX-luc
siKLF5
siERβ

Figure_6

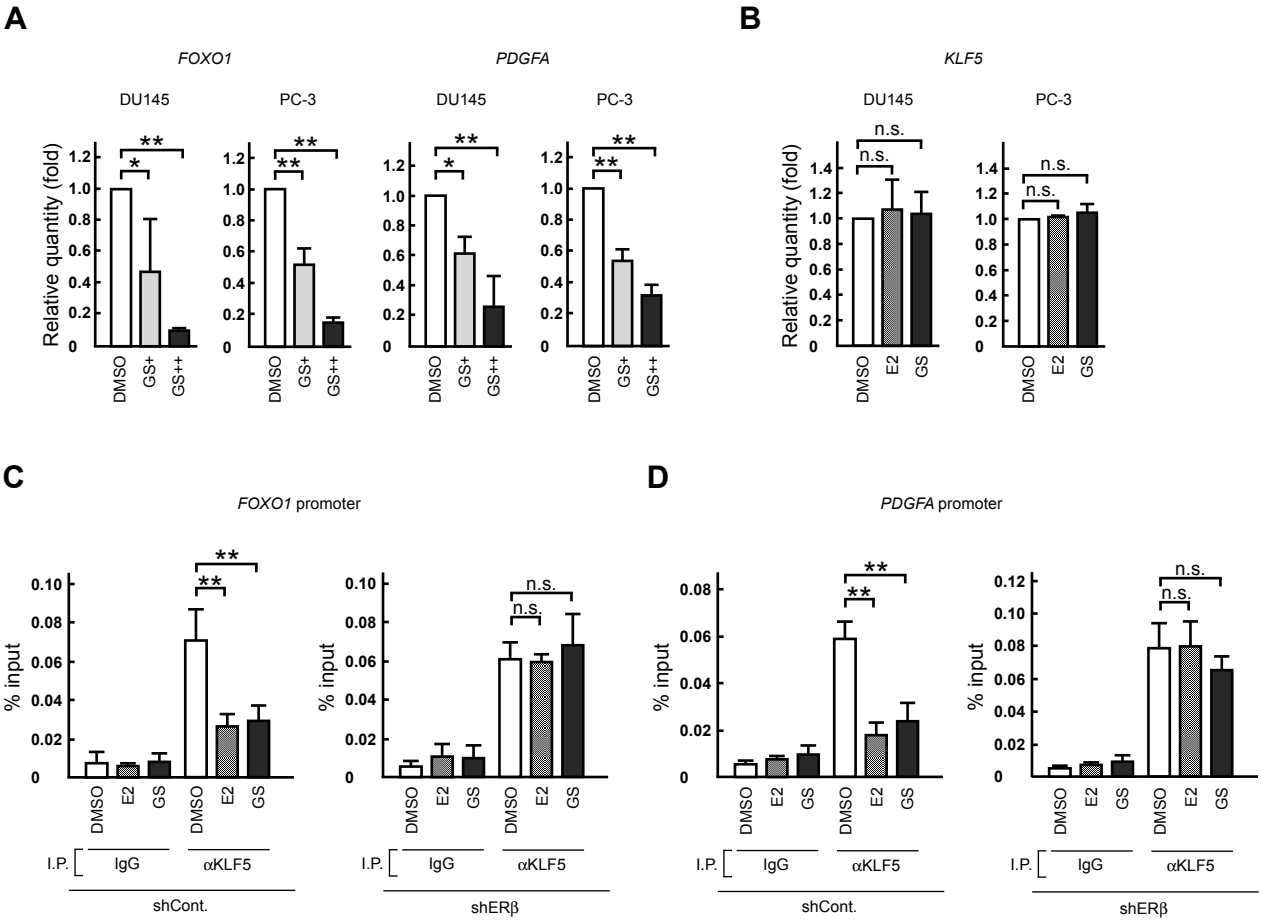
A
FOXO1
PDGFA
DU145
PC-3
DU145
PC-3
Relative quantity (fold)
DMSO
GS+
GS++
B
KLF5
DU145
PC-3
n.s.
Relative quantity (fold)
DMSO
E2
GS
C
FOXO1 promoter
% input
DMSO
E2
GS
I.P.
IgG
αKLF5
shCont.
shERβ
n.s.
D
PDGFA promoter
% input
shCont.
shERβ

Figure_7

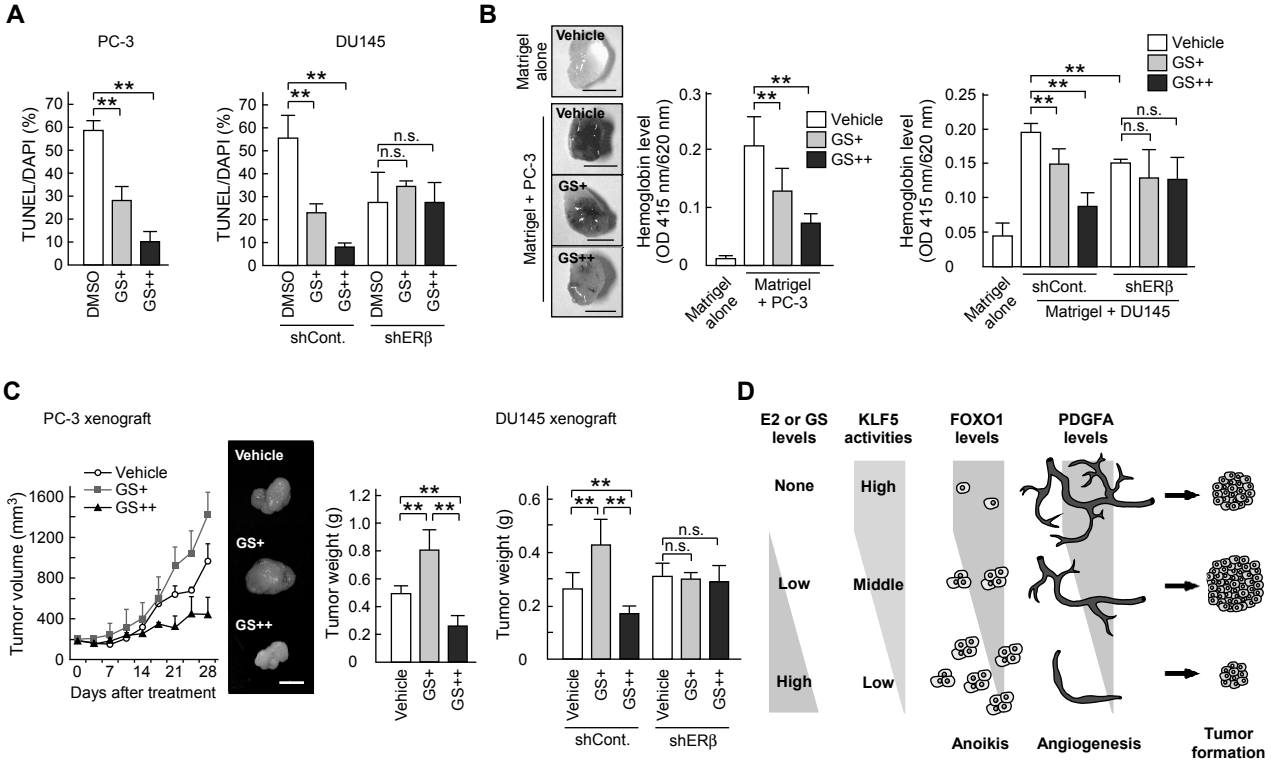
A
PC-3
DU145
TUNEL/DAPI (%)
DMSO
GS+
GS++
shCont.
shERβ
n.s.
B
Matrigel alone
Matrigel + PC-3
Vehicle
GS+
GS++
Hemoglobin level (OD 415 nm/620 nm)
Matrigel + DU145
C
PC-3 xenograft
DU145 xenograft
Tumor volume (mm3)
Days after treatment
Tumor weight (g)
D
E2 or GS levels
KLF5 activities
FOXO1 levels
PDGFA levels
None
Low
High
Middle
Anoikis
Angiogenesis
Tumor formation

Figure_8